Variable sample temperature scanning superconducting quantum interference device microscope

J. R. Kirtley[a] and C. C. Tsuei
IBM T. J. Watson Research Center, P.O. Box 218, Yorktown Heights, New York 10598

K. A. Moler
Department of Applied Physics, Stanford University, Stanford, California 94305

V. G. Kogan and J. R. Clem
Ames Laboratory and Physics Department ISU, Ames, Iowa 50011

A. J. Turberfield
Department of Physics, University of Oxford, Clarendon Laboratory Parks Road, Oxford OX13PU, United Kingdom

(Received 10 March 1999; accepted for publication 4 May 1999)

We demonstrate a design for a scanning superconducting quantum interference device (SQUID) microscope in which the sample temperature can be varied over a large range. In this design, both sample and SQUID are in the same vacuum space, separated by a few microns. By firmly anchoring the SQUID to a low-temperature bath, the sample temperature can be changed while the SQUID remains superconducting. This allows magnetic imaging at varying sample temperatures with micron-scale spatial resolution and the sensitivity of a low-T_c SQUID. We demonstrate this approach by imaging the temperature dependence of Abrikosov vortices in thin films of the high-temperature superconductor $YBa_2Cu_3O_{7-\delta}$. We extract the in-plane penetration depth $\lambda_{ab}(T)$ in our samples from these measurements. © *1999 American Institute of Physics.* [S0003-6951(99)04026-7]

The scanning superconducting quantum interference device (SQUID) microscope is a powerful tool for imaging sample magnetic fields.[1] This tool has the advantage of high sensitivity, but the disadvantages of relatively modest spatial resolution, and the requirement that the SQUID sensor be cooled. This means that either the sample must also be cold, or that there must be a thermally insulating region between the SQUID and sample. It is desirable to minimize the spacing between the SQUID and sample, because this spacing limits the ultimate spatial resolution and sensitivity of the instrument. Recently, several scanning SQUID microscopes have been built which image room-temperature samples using a thin membrane to isolate high-T_c sensors in a cryogenic environment from room-temperature samples.[2–4] Sample–SQUID spacings as small as 15 μm have been achieved in these instruments. However, for certain applications it is desirable to vary the sample temperature. It is also often desirable to reduce the SQUID–sample spacing further than is possible with a physical barrier between the sample and the cryogenic environment.

We have built a variable sample temperature scanning SQUID microscope with both the SQUID and the sample in the same space (see Fig. 1), with the insulation between them provided by vacuum.[5] Since in this configuration there is no fundamental limit to how small the spacing between the SQUID and sample need be, this optimizes the sensitivity and spatial resolution of the instrument. In this letter, data were taken with a SQUID–sample spacing of about 4 μm.

As in previous instruments,[6] we use a low-T_c Nb–AlO_x–Nb SQUID with an integrated pickup loop. Three room-temperature dc motors scan the sample relative to the SQUID using a pivoted lever rod. The SQUID is etched and polished so that the pickup loop is less than a loop diameter from the sharpened tip of the silicon substrate, which is mounted on a flexible cantilever. Both SQUID and sample orientations are adjusted independently before cooling, so that the SQUID substrate plane is tilted at an angle of a few degrees from the sample plane, and the sample plane is aligned parallel to the scan plane. After alignment, the microscope is inserted in a stainless-steel vacuum can and cooled in a He^4 bath. He^3, which is easier to pump at low temperatures than He^4, is used as an exchange gas.

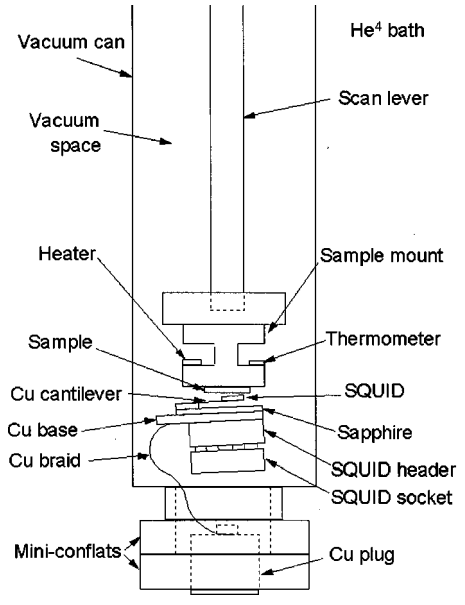

FIG. 1. Schematic drawing of our variable temperature scanning SQUID microscope.

[a]Electronic mail: kirtley@us.ibm.com

Good thermal contact between the SQUID and the He^4 bath is maintained through two 1 mm diam silver-plated copper braids. The copper braids are clamped to a copper plug that passes through the vacuum can into the He^4 bath. The other ends of the braids are clamped to a silver-plated copper base on the SQUID header assembly. A sapphire substrate is glued with silver epoxy to the copper base, the copper cantilever is glued with silver epoxy to the sapphire, and the SQUID is attached to the cantilever with a thin coating of varnish. The SQUID is wire bonded using aluminum wires, which are heat sunk to the sapphire substrate through electroplated copper contacts. Since the silicon substrate, copper, and silver are all excellent thermal conductors at low temperature, we estimate that the thermal resistance between the SQUID and the He^4 bath is dominated by the cantilever resistance. With the He^3 exchange gas pumped out, the thermal conductance between the SQUID and sample should be limited by radiation. In this case, the temperature of the SQUID is given by $T_{\mathrm{SQUID}}=T_{\mathrm{bath}}+\sigma A(T^4_{\mathrm{sample}}+T^4_{\mathrm{bath}}-T^4_{\mathrm{SQUID}})/G$, where $\sigma=5.67\times10^{-12}$ W/cm^2 K^4 is the Stefan–Boltzmann constant, A is an effective area of the cantilever, and G is the cantilever thermal conductance. We estimate the cantilever thermal conductance at low temperatures to be about 2.5×10^{-3}W/K and $A=0.05\,\mathrm{cm}^2$. Since the SQUID will continue to function up to about 8 K, this means that in principle the sample temperature can be over 400 K while still operating the SQUID. In practice, there is parasitic thermal conductance between the SQUID and sample (as evidenced by a linear relation between our measured SQUID and sample temperatures). This is possibly due to thermal conduction through the wires to both SQUID header and sample from the top of the microscope. This parasitic conductance limits our sample temperatures to below 150 K before the SQUID is driven normal. However, this is a useful temperature range, which may be extended further by, for example, carefully heat sinking of the leads.

As a demonstration of this technique, we present SQUID microscope measurements of the temperature dependence of individual Abrikosov vortices trapped in a 300-nm-thick, c-axis up films of $YBa_2Cu_3O_{7-\delta}$ (YBCO). Similar measurements, with much lower field sensitivities, have been made previously using Hall bars[7–9] and magnetic force microscopy.[10,11] For these measurements we used a SQUID with a relatively large pickup loop, a square 17.8 μm on a side. This loop size was chosen to make the measurements less sensitive to errors in the positioning of the tip relative to the vortex. There is no reason that smaller loop sizes cannot be used. Figure 2(a) shows a typical magnetic image of an individual Abrikosov vortex. Superimposed on this image is a scaled schematic of the pickup loop geometry. For all the measurements presented here, the vortex images are resolution limited, since the in-plane penetration depth is shorter than the size of the pickup loop. Nevertheless, as λ_{ab} becomes large compared to the film thickness, it can be quantitatively determined from the peak height, even though λ_{ab} is small compared to the pickup loop. The open circles in Fig. 2(b) are cross sections through the center of the vortex at various temperatures. The lines in Fig. 2(b) are fits to these cross sections, using the in-plane penetration depth λ_{ab} as a fitting parameter.

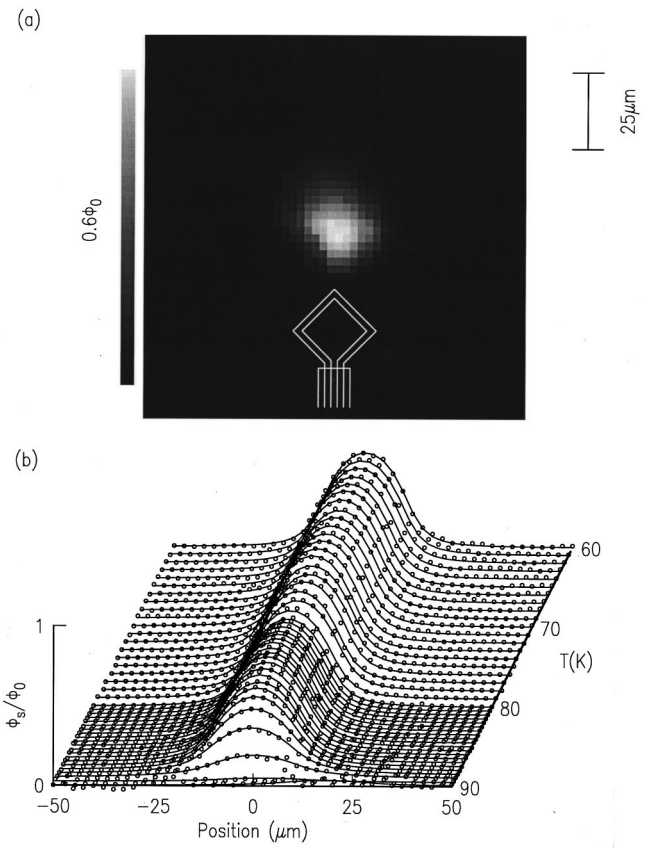

FIG. 2. (a) Scanning SQUID microscope image of a single Abrikosov vortex in a thin film of $YBa_2Cu_3O_{7-\delta}$. (b) The open circles are cross-sectional data through the center of a vortex, for a number of temperatures. The lines are fits to the data.

Our fits are made as follows: We model a vortex centered at $x=y=0$ with its axis oriented parallel to the z axis (normal to the plane) of a superconducting film of arbitrary thickness d with the center of the film at $z=0$. Solutions for the magnetic field and supercurrent generated by a vortex are given in Ref. 12 for a vortex whose core size is characterized by a variational core radius parameter ξ_v.[13] In the present experiments, the resolution of the SQUID microscope is such that details of the vortex magnetic field on the scale of the coherence distance cannot be resolved. We, therefore, can safely use the solution in the limit $\xi_v\to0$ for the z component of the magnetic field above the surface of the superconductor. This result, also obtained by Chang *et al.*,[7] can be derived as in Ref. 14 by solving London's equations for the field inside the superconductor and matching the result to a solution of Maxwell's equations in the vacuum outside the sample. The solution is

$$h_z(\mathbf{r},z)=\frac{\phi_0}{(2\pi\lambda_{ab})^2}\int d^2\mathbf{k}e^{i\mathbf{k}\cdot\mathbf{r}}\frac{e^{k(d/2-z)}}{\alpha[\alpha+k\coth(\alpha d/2)]}, \tag{1}$$

where $\mathbf{r}=\{x,y\}$, $\mathbf{k}=\{k_x,k_y\}$, $k=\sqrt{k_x^2+k_y^2}$, and $\alpha=\sqrt{k^2+\lambda_{ab}^{-2}}$.

Note that this solution is independent of the out-of-plane penetration depth λ_c because the vortex currents flow parallel to the plane. It reduces to the Pearl results for a half space[15] as $d\to\infty$, and to the thin-film limit as $d\to0$.[16,17] The flux through the SQUID pickup loop is obtained from Eq. (1)

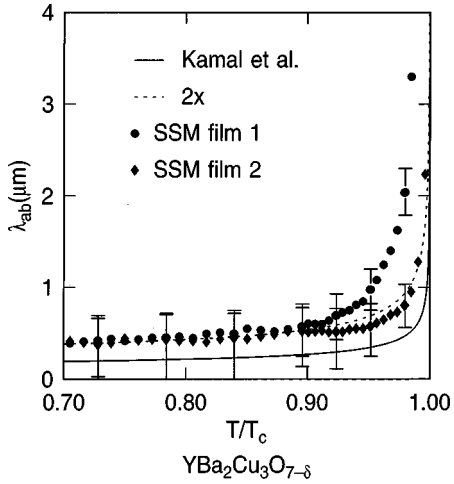

FIG. 3. Comparison of values for the in-plane penetration depth derived from fitting scanning SQUID microscope (SSM) images for two different YBCO films, with microwave data from Ref. 18 for a single crystal of YBCO.

by numerically integrating over the known geometry of the pickup loop. The fits displayed in Fig. 2(b) had four parameters: λ_{ab}; z_0, the height of the pickup loop above the sample surface; x_0, the center position of the vortex; and $\phi_{\rm off}$, an offset flux. While making the cross-sectional measurements in Fig. 2 the sample was moved towards the SQUID until contact was made, as judged by a sharp decrease in the critical current of the SQUID. Then, the sample was backed off by 1 μm for the measurement. We are, therefore, confident that the sample–SQUID spacing was constant within ± 1 μm. However, because of uncertainties in the tip–sample geometry at low temperatures, we are less certain of the absolute value of this spacing. We estimate that this spacing was between 2 and 5 μm. We fit our data using $z_0 = 3.5\ \mu m$ and assign error bars by repeating these fits using $z_0 = 2$ and 5 μm. The fits, displayed in Fig. 2(b) for one of our films (film 2 in Fig. 3 below), are good, with no change in the quality of the fit apparent throughout the measured temperature range.

The solid symbols in Fig. 3 show fit values for λ_{ab} for two different $YBa_2Cu_3O_{7-\delta}$ thin films. These films were grown epitaxially, oriented c-axis up, on $SrTiO_3$ using laser ablation. They had a $T_c(R=0) = 91.3$ K with a midpoint of the resistive transition temperature of 91.8 K. Also shown for comparison as the solid line are data for λ_{ab} for a high-quality YBCO single crystal taken from the work of Kamal *et al.*[18] The dashed line is this data, with λ_{ab} multiplied by a factor of 2. This scaled line agrees with our fits to within our assigned error bars, showing an approximately similar temperature scaling. Clearly, the two films, although nominally identical, and grown on the same substrate, have temperature dependences near T_c that are different from each other. We speculate that this may be due to the fact that film 1 had been photolithographically patterned and repeatedly thermally cycled, whereas film 2 was freshly made for these measurements. Our absolute values are somewhat higher than other estimates for YBCO thin films,[9,10,19–21] perhaps because of our uncertainty in the value of the tip height. However, there may also be a more interesting difference between our temperature dependence of λ_{ab} and that of Kamal *et al.* We note that our films had T_c's of 91 K and transition widths of 1 K, whereas the single crystals had T_c's of nearly 94 K and transition widths of about 0.25 K.

Measurements of the temperature dependence of the penetration depth on a local scale may provide a test of the quality of thin superconducting films that is more stringent than conventional bulk measurements. It is also of interest to compare measurements made with our technique with measurements using microwave techniques on the same sample to test, for example, for the possibility of vortex motion close to T_C.

In conclusion, we have demonstrated a scanning SQUID microscope which can vary the sample temperature well above the critical temperature of the SQUID, with little sacrifice in spatial resolution or sensitivity. Such instruments should have a number of applications in areas well beyond the study of superconductors.

We would like to thank J. R. Rozen for technical assistance; and M. B. Ketchen for the design, and M. Bhushan for the fabrication of the SQUIDs used in this study. The authors would also like to thank S. Kamal and W. N. Hardy for providing their data and for useful discussions.

[1] J. R. Kirtley and J. P. Wikswo, *Annual Reviews of Materials Science* (Annual Reviews, Palo Alto, CA, 1999), Vol. 29.
[2] R. C. Black, Ph.D. thesis, University of Maryland, 1995.
[3] T. S. Lee, E. Dantsker, and J. Clarke, Rev. Sci. Instrum. **67**, 4208 (1996).
[4] T. S. Lee, Y. R. Chemla, E. Dantsker, and J. Clarke, IEEE Trans. Appl. Supercond. **50**, 3147 (1997).
[5] M. J. Ferrari, M. Johnson, F. C. Wellstood, J. Clarke, P. A. Rosenthal, R. H. Hammond, and M. R. Beasley, Appl. Phys. Lett. **53**, 695 (1988).
[6] J. R. Kirtley, M. B. Ketchen, C. C. Tsuei, J. Z. Sun, W. J. Gallagher, L. S. Yu-Jahnes, A. Gupta, K. G. Stawiasz, and S. J. Wind, Appl. Phys. Lett. **66**, 1138 (1995).
[7] A. M. Chang, H. D. Hallen, L. Harriott, H. F. Hess, H. L. Kao, J. Kwo, R. E. Miller, R. Wolfe, J. van der Ziel, and T. V. Chang, Appl. Phys. Lett. **61**, 1974 (1992).
[8] A. M. Chang, H. D. Hallen, H. F. Hess, H. L. Kao, J. Kwo, A. Sudbo, and T. Y. Chang, Europhys. Lett. **20**, 645 (1992).
[9] A. Oral, S. J. Bending, R. G. Humphreys, and M. Henini, J. Low Temp. Phys. **105**, 1135 (1996).
[10] A. Moser, H. J. Hug, I. Parashikov, B. Stiefel, O. Fritz, H. Thomas, A. Baratoff, H. J. Guntherodt, and P. Chaudhari, Phys. Rev. Lett. **74**, 1847 (1995).
[11] C. W. Yuan, Z. Zheng, A. L. de Lozanne, M. Tortonese, D. A. Rudman, and J. N. Eckstein, J. Vac. Sci. Technol. B **14**, 1210 (1996).
[12] J. R. Clem, in *Inhomogeneous Superconductors - 1979*, edited by D. U. Gubser, T. L. Francavilla, S. A. Wolf, and J. R. Leibowitz (American Institute of Physics, New York, 1980), p. 245.
[13] J. R. Clem, J. Low Temp. Phys. **18**, 427 (1975).
[14] J. R. Kirtley, V, Kogan, J. R. Clem, and K. A. Moler, Phys. Rev. B **59**, 4343 (1999).
[15] J. Pearl, J. Appl. Phys. **37**, 4139 (1966).
[16] J. Pearl, Appl. Phys. Lett. **5**, 65 (1964).
[17] P. G. de Gennes, *Superconductivity of Metals and Alloys* (Benjamin, New York, 1966), p. 60.
[18] S. Kamal, R. Liang, A. Hosseini, D. A. Bonn, and W. N. Hardy, Phys. Rev. B **58**, R8933 (1998).
[19] S. Hensen, G. Müller, C. T. Rieck, and K. Scharnberg, Phys. Rev. B **56**, 6237 (1997).
[20] S. Djordjevic, L. A. de Vaulchier, N. Bontemps, J. P. Vieren, Y. Guldner, S. Moffat, J. Preston, X. Castel, M. Guilloux Viry, and A. Perrin, Eur. Phys. J. B **5**, 847 (1998).
[21] A. G. Sun, S. H. Han, A. S. Katz, D. A. Gajewski, M. B. Maple, and R. C. Dynes, Phys. Rev. B **52**, R15731 (1995).